

# **Photoactivated plasmonic nanohybrid fibers with prolonged trapping of excited charge carriers for SERS analysis of biomolecules**

Arti Sharma, <sup>a#</sup> Tripti Ahuja, <sup>b#</sup> Jatin Yadav, <sup>a</sup> Shubhangi Majumdar, <sup>a</sup> Soumik Siddhanta<sup>a\*</sup>

- a. Indian Institute of Technology, Hauz Khas, New Delhi
- b. Presently at Indian Institute of Technology, Kanpur, Uttar Pradesh
- # These authors have contributed equally

## Synthesis of Silver Nanoparticles

Silver nanoparticles are prepared by using the classical Lee Meisel<sup>1</sup> approach. 10 mg of AgNO<sub>3</sub> salt was added to the 50 mL of Milli-Q water. 1% of sodium tribasic citrate aqueous solution was added to the above mixture on boiling. The synthesized nanoparticles are characterized by UV-visible spectroscopy.

## Transient Absorption Spectroscopy Experiments

The samples dispersed in a solvent were held in a 2 mm quartz cuvette and stirred constantly by a magnetic stirrer during the measurements. For transient measurements, 410 nm was used as the pump wavelength, and sapphire crystal for visible range white light as a probe.

## Calculations of Decay Time

The transient decays were fitted by using equation (1), deconvoluting instrument response function with the help of Surface Xplorer software<sup>2</sup>, and the averaged lifetimes were calculated according to equation (2). Where  $\Delta A(\lambda, t)$  is the observed change in absorbance at time  $t$  and wavelength  $\lambda$ ,  $A$  is amplitude, and  $\tau$  is the time constant  $i^{\text{th}}$  components.

$$\Delta A(\lambda, t) = A_0 + \sum_i A_i e^{-\frac{t}{\tau_i}} \quad (1)$$

$$\langle \tau \rangle = \frac{\sum_i A_i \tau_i}{\sum_i A_i} \quad (2)$$

## Calculation of Full-width and Half maxima and band gap of AINFs

Full-Width and half-maxima are calculated by fitting the UV-visible curve using the Gaussian function in origin software. The band gap for the AINFs is calculated by using UV-vis spectroscopy.

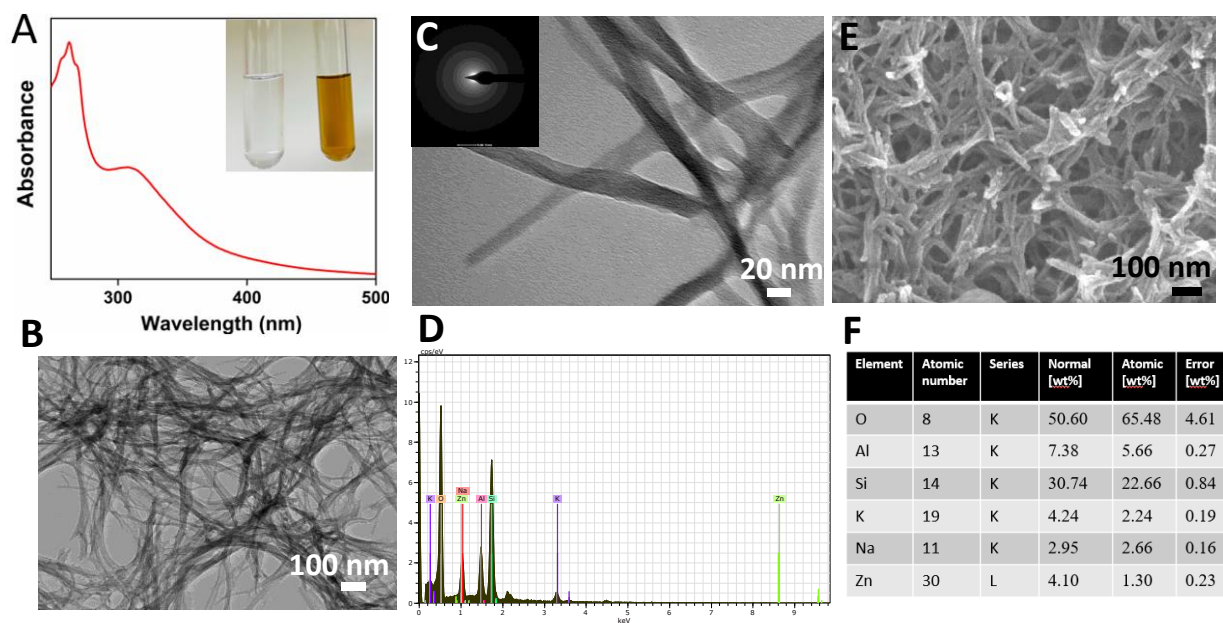


**Figure S1:** **A.** UV-visible spectra of AlNFs in ethylene glycol, the inset figure shows the color change of  $\text{Al}(\text{NO}_3)_3 \cdot 9\text{H}_2\text{O}$  from colorless to yellow in EG before and after microwave heating. **B.** TEM image of the AlNFs at 100 nm scale. **C.** HR-TEM characterization of AlNFs, the inset figure shows the SAED pattern of the fibers indicating the amorphous nature of AlNFs. **D.** Table representing the elemental composition and atomic weight % of the elements present in AlNFs. **E.** Fe-SEM characterization for the surface morphology of AlNFs at 100 nm scale. **F.** EDAX analysis of a specific region of AlNFs from Figure C.

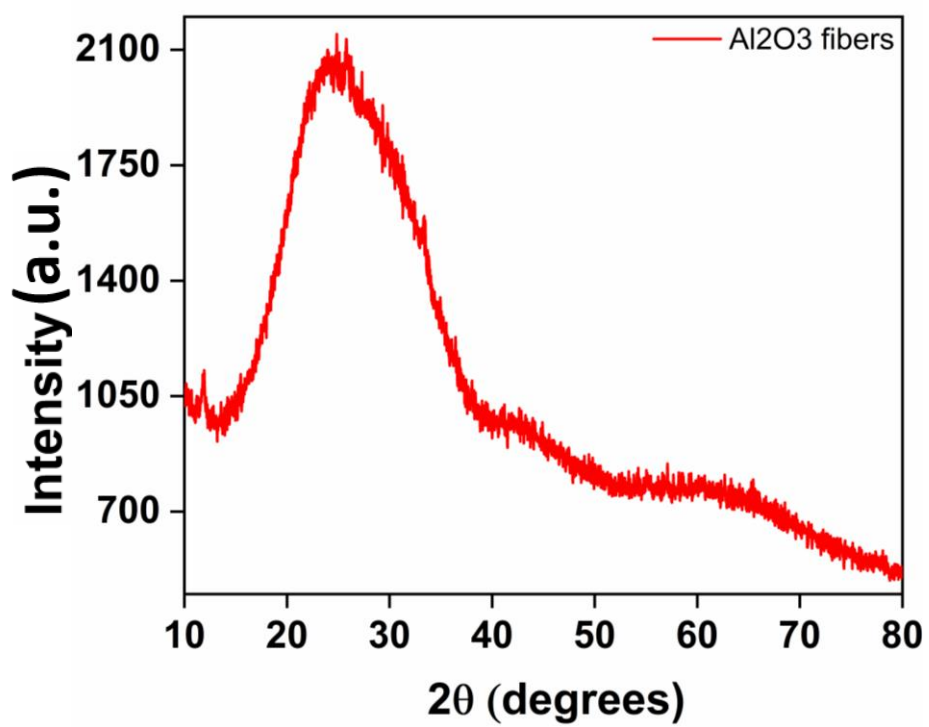


**Figure S2:** Diffractogram of Alumina nanofibers. The broad peak shows the amorphous nature of the alumina nanofibers.

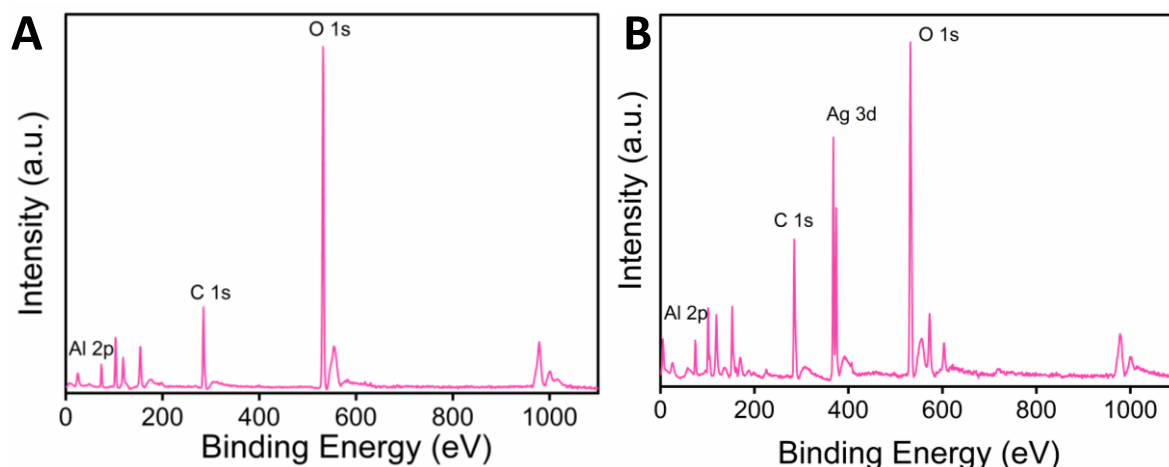


**Figure S3:** XPS Survey spectra for A) AlNFs and B) Ag-AlNFs.

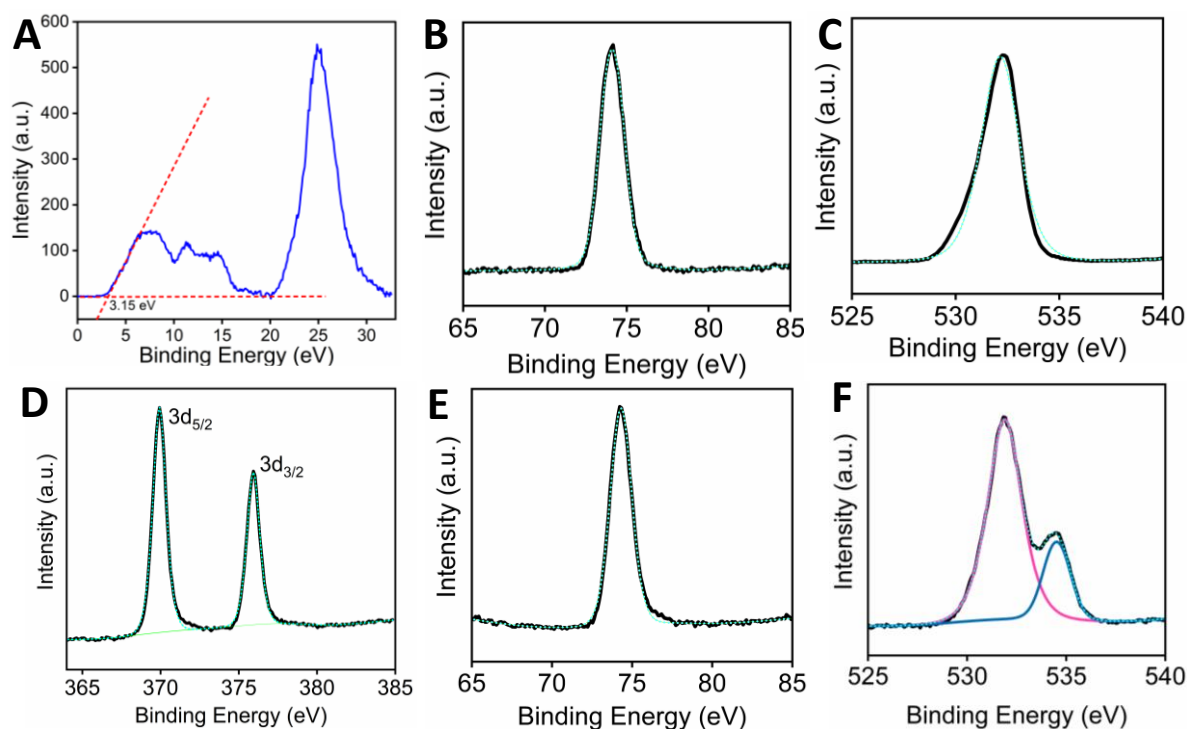


**Figure S4:** **A.** Valence band XPS spectra of AlNFs, the tangent drawn to the peaks gives the value of the valence band edge.<sup>3</sup> **B.** Al 2p XPS spectra of Al<sub>2</sub>O<sub>3</sub> nanofibers (74.1 eV).<sup>4</sup> **C.** Oxygen 1s XPS spectra of Al<sub>2</sub>O<sub>3</sub> nanofibers (532.3 eV).<sup>5</sup> **D.** Ag 3d XPS spectra at 369.5 eV and 375.98 eV of Ag-AlNFs hybrid structures which further confirms the formation of silver nanoparticles in AlNFs.<sup>6</sup> **E** Al 2p peak XPS spectra of Ag-AlNFs at 74.2 eV. **F** Oxygen 1s spectra of Ag-AlNFs at 531.9 eV and extra peak at 534.5 which might be due to water vapour. (Peak fitting was done using Gaussian-Lorentz function in B, C, D, E and F spectra. The black curve shows the raw data, dotted cyan color shows the fitted data)

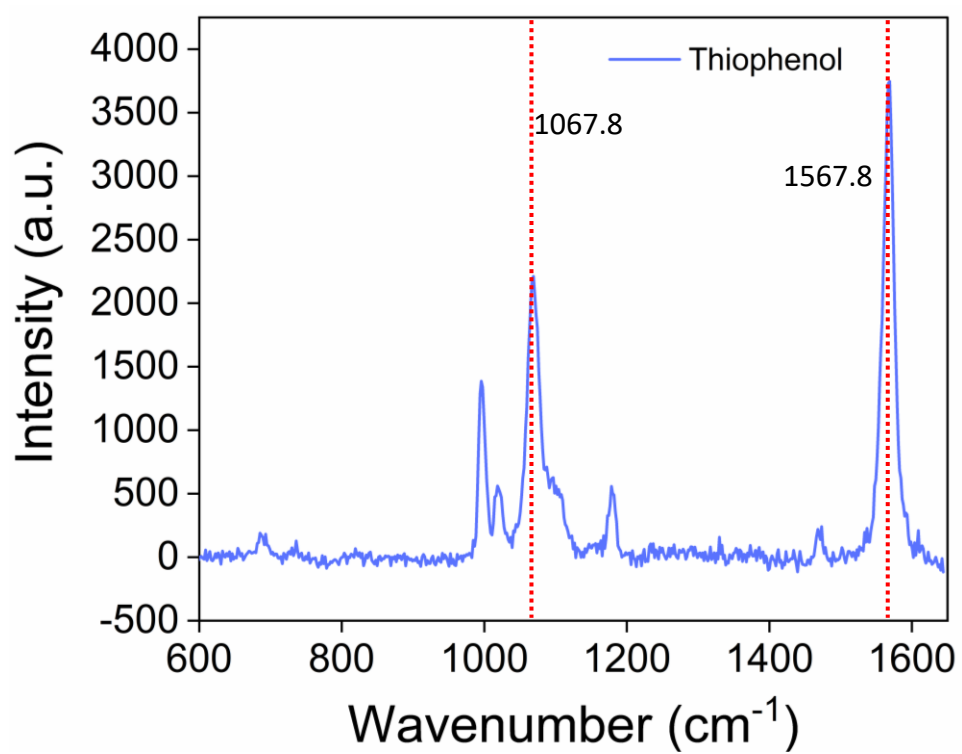


**Figure S5:** Shows the SERS spectra of thiophenol. The peak 1067.8 and 1567.8 cm<sup>-1</sup> were chosen for the Raman mapping for both UV-exposed and non-exposed Ag-AINFs.

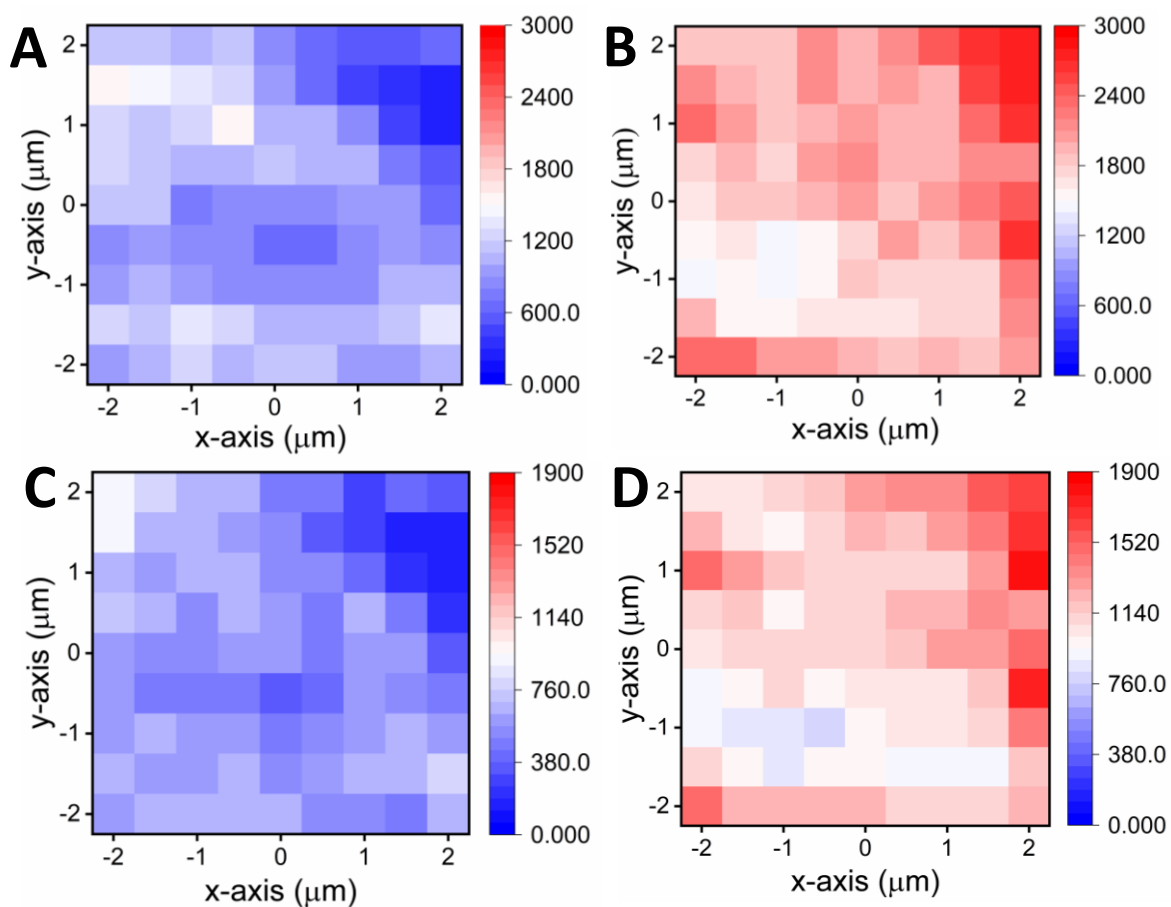


**Figure S6:** **A and B** Shows the SERS mapping of the 1567.8 cm<sup>-1</sup> peak of the thiophenol (10<sup>-6</sup> M) compound adsorbed over non-UV-exposed Ag-AINFs substrate and UV exposed Ag-AINFs, respectively. The scale bar on the right shows the enhanced SERS intensity of the thiophenol in UV exposed sample (**shown in red color**) and less intensity in the case of the non-UV-exposed sample (**shown in blue color**), **C and D** Show the SERS mapping of thiophenol at peak 1067.8 cm<sup>-1</sup> over non-UV-exposed Ag-AINFs substrate and UV-exposed Ag-AINFs respectively.

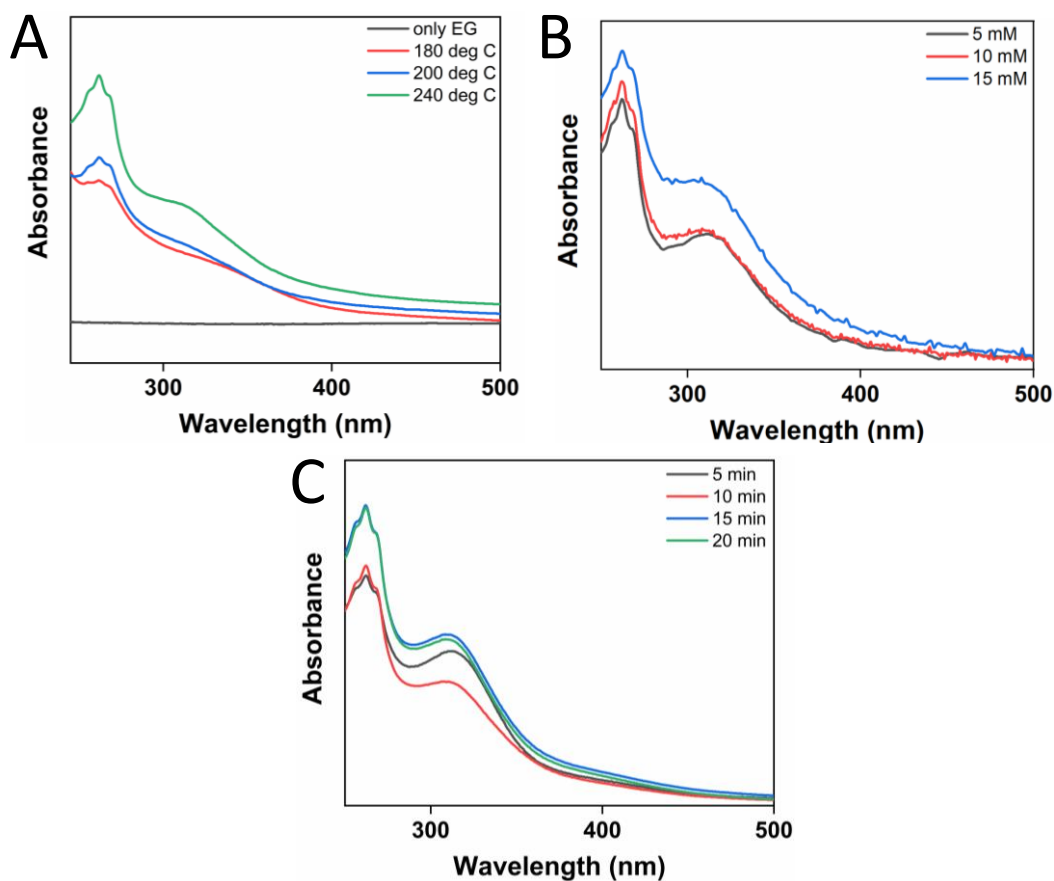


**Figure S7:** UV-vis spectra showing **A.** Optimization of temperature. The higher the temperature the more is the increase in the intensity of the UV-vis peak observed which indicates more formation of the AINFs. **B.** Optimization of the concentration. The greater concentration of  $\text{Al}(\text{NO}_3)_3 \cdot 9\text{H}_2\text{O}$  salt indicates more formation of fibers, however to prevent more wastage of chemical 5 mM concentration was chosen and **C.** Time for the synthesis of AINFs in ethylene glycol solvent.

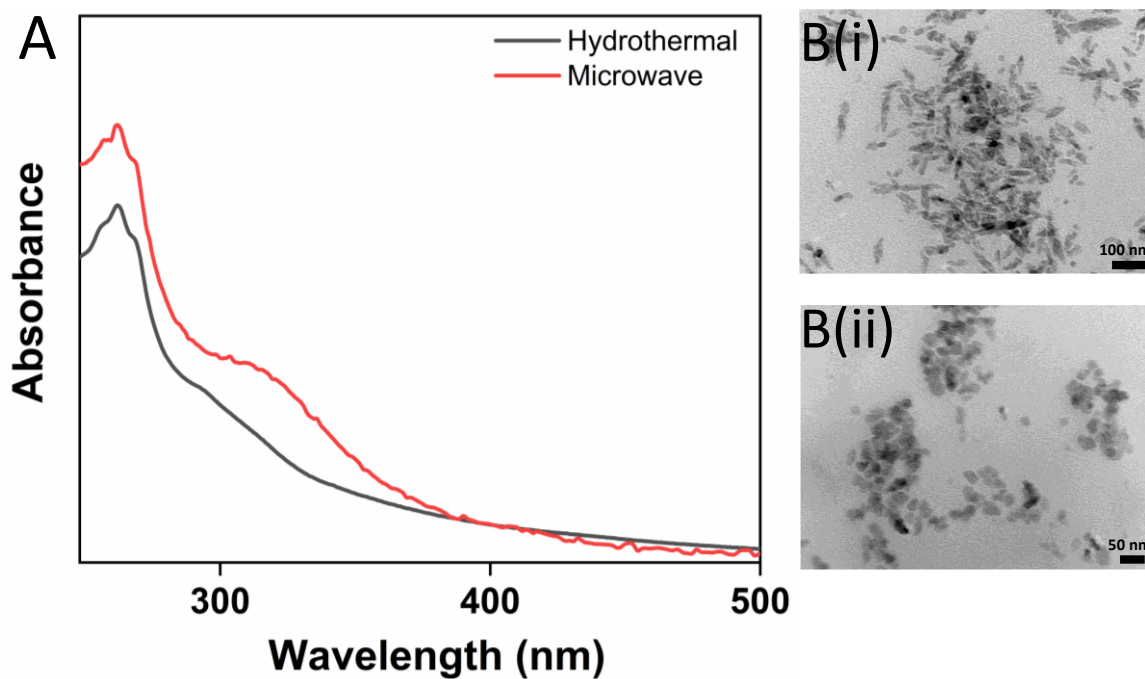


**Figure S8:** **A.** UV-vis spectra of ALNFs in ethylene glycol in the presence of MW heating (red) and hydrothermal heating (black) **B.** (i, ii) TEM images of ALNFs prepared via hydrothermal at different scales 100 nm and 50 nm.

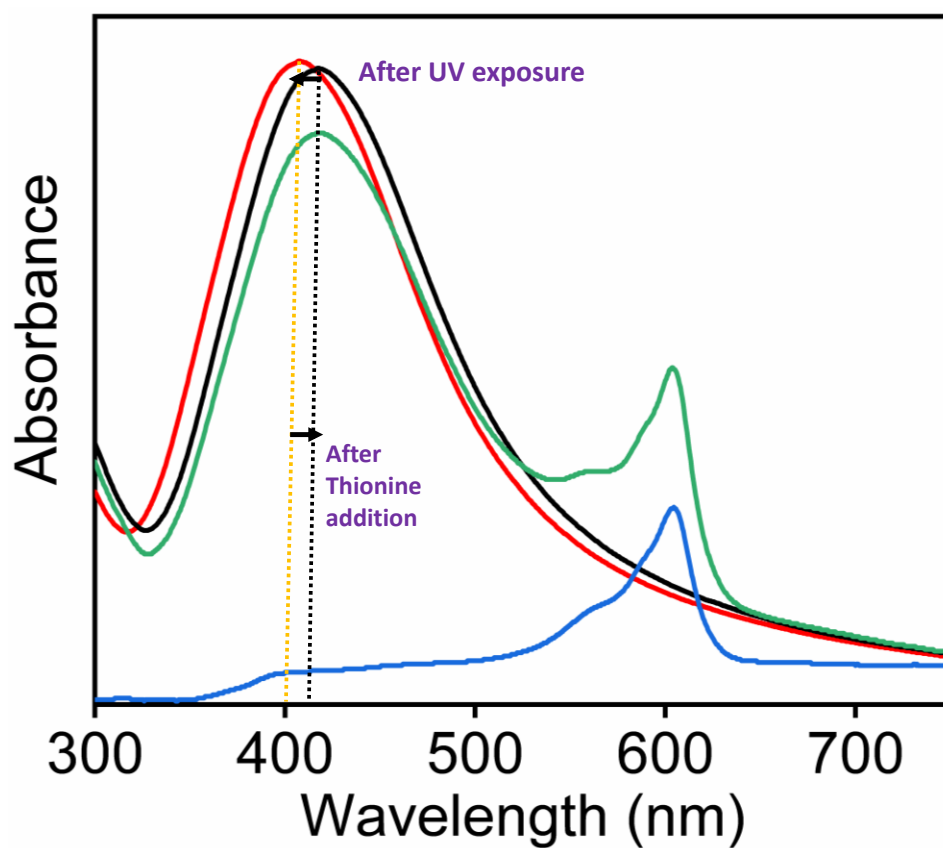


**Figure S9:** Shows the UV-vis spectra of Nanoparticles before (black color) and after UV exposure (red color). The addition of thionin dye shows further reversibility of the electron transfer process, which shifts the plasmonic peak to its original position (green color). UV-vis spectrum of only thionin compound is shown in blue color.

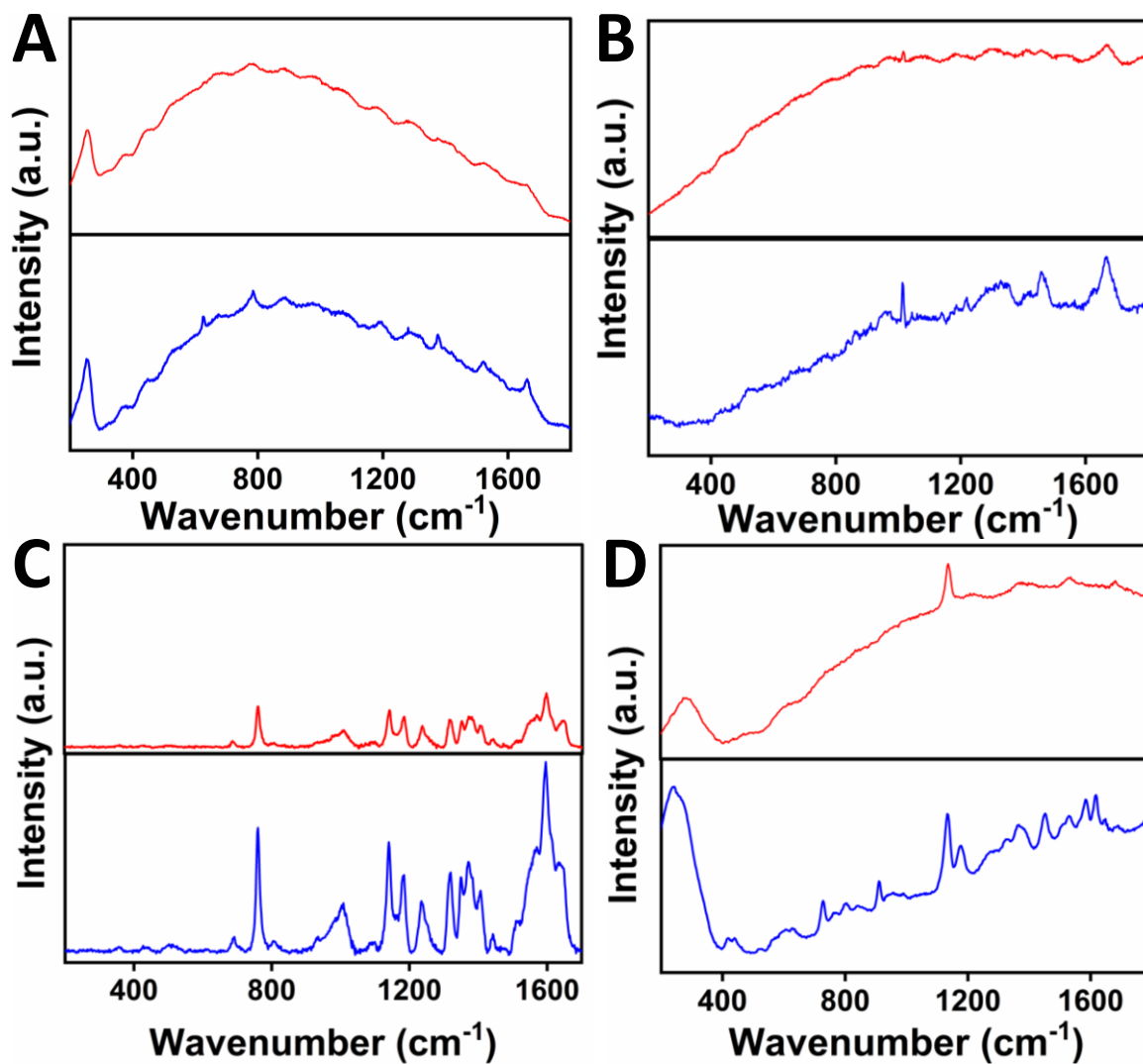


**Figure S10:** Averaged Raman spectra of A. Lysozyme, B. BSA, C. Myoglobin, and D. DNA on Ag-AINFs both in the presence (shown in blue) and absence of UV exposure (red) at different locations.

## REFERENCES

- (1) Lee, P. C.; Meisel, D. Adsorption and surface-enhanced Raman of dyes on silver and gold sols. *The Journal of Physical Chemistry* **1982**, *86* (17), 3391-3395.
- (2) Niedzwiedzki, D. M.; Sullivan, J. O.; Polívka, T.; Birge, R. R.; Frank, H. A. Femtosecond time-resolved transient absorption spectroscopy of xanthophylls. *The Journal of Physical Chemistry B* **2006**, *110* (45), 22872-22885.
- (3) Filatova, E. O.; Konashuk, A. S. Interpretation of the changing the band gap of Al<sub>2</sub>O<sub>3</sub> depending on its crystalline form: connection with different local symmetries. *The Journal of Physical Chemistry C* **2015**, *119* (35), 20755-20761.
- (4) Alshehri, A. H.; Mistry, K.; Nguyen, V. H.; Ibrahim, K. H.; Muñoz-Rojas, D.; Yavuz, M.; Musselman, K. P. Quantum-Tunneling Metal-Insulator-Metal Diodes Made by Rapid Atmospheric Pressure Chemical Vapor Deposition. *Advanced Functional Materials* **2019**, *29* (7), 1805533.
- (5) Yang, C.-S.; Kim, J.-S.; Choi, J.-W.; Kwon, M.-H.; Kim, Y.-J.; Choi, J.-G.; Kim, G.-T. XPS study of aluminum oxides deposited on PET thin film XPS study of aluminum oxides deposited on PET thin film. *Journal of Industrial and Engineering Chemistry* **2000**, *6* (3), 149-156.
- (6) Bera, S.; Gangopadhyay, P.; Nair, K. G. M.; Panigrahi, B. K.; Narasimhan, S. V. Electron spectroscopic analysis of silver nanoparticles in a soda-glass matrix. *Journal of electron spectroscopy and related phenomena* **2006**, *152* (1-2), 91-95.